

UC Berkeley
SEMM Reports Series

Title

Finite Deformation Inverse Design Modeling with Temperature Changes, Axis-Symmetry, and Anisotropy

Permalink

<https://escholarship.org/uc/item/1304p3pk>

Author

Govindjee, Sanjay

Publication Date

1999

REPORT NO.
UCB/SEMM-1999/01

STRUCTURAL ENGINEERING
MECHANICS AND MATERIALS

FINITE DEFORMATION INVERSE DESIGN
MODELING WITH TEMPERATURE CHANGES,
AXIS-SYMMETRY, AND ANISOTROPY

BY

SANJAY GOVINDJEE

JANUARY 1999

DEPARTMENT OF CIVIL ENGINEERING
UNIVERSITY OF CALIFORNIA
BERKELEY, CALIFORNIA

Finite Deformation Inverse Design Modeling with Temperature Changes, Axis-Symmetry and Anisotropy

Sanjay Govindjee ^{a,1}

*^aStructural Engineering, Mechanics, and Materials
Department of Civil and Environmental Engineering
University of California, Berkeley
Berkeley, CA 94720-1710*

Abstract

In the manufacture and use of elastomeric components inverse design methods are gaining popularity. These methods allow for the computation of the to-be-manufactured shape of an elastomeric component when geometric and load constraints are specified on a deformed in-use part. Formulations are presently available for the basic cases of 2-D plane and 3-D isothermal hyperelasticity. This report extends the inverse design methodology of Govindjee & Mihalic (1996) and Govindjee & Mihalic (1998) to include the possibility of differing temperatures in the to-be-manufactured configuration and the use configuration, the possibility of axis-symmetric geometries, and the possibility of transverse isotropy. Orthotropic material behavior is also considered.

Key words: Inverse Design, Thermoelasticity, Anisotropy, Axis-Symmetry

1 Introduction

A problem encountered in the design of finitely deformed elastomeric parts is one in which the initial undeformed shape of a body is unknown and the final deformed shape, applied Cauchy tractions, and displacement boundary conditions are known. The problem being to compute the undeformed shape. Problems of this type were first examined by Euler (1744) for a cantilevered elastica. Recently Govindjee & Mihalic (1996) and Govindjee & Mihalic (1998) have developed computational methods for solving such problems in continua.

¹ Assistant Professor of Civil Engineering, govindjee@ce.berkeley.edu

These works provide for methods appropriate to 2-D plane and 3-D hyperelastic compressible and quasi-incompressible materials. In practical applications, the manufacturing processes occur at different temperatures from those where the components will be used. Thus it is important to extend these methods to account for temperature changes. Further, elastomeric components are often layered with anisotropic materials for stiffening. Thus these methods should also be extended to incorporate anisotropic effects. It is also noted that for economy of computation it is desirable to treat axis-symmetric cases separate from 3-D continua. These three extensions of the inverse design method are described in the following sections.

2 Thermoelasticity

The point of departure for hyperelastic thermoelasticity is the seminal work of Chadwick (1974). If one assumes for simplicity a constant heat capacity, then the Helmholtz free energy function can be expressed as

$$\Psi(\mathbf{F}, T) = \frac{T}{T_o} \Psi_o(\mathbf{F}) + \left(1 - \frac{T}{T_o}\right) e_o(\mathbf{F}) + \bar{c} \left(T - T_o - T \ln \frac{T}{T_o}\right), \quad (1)$$

where \mathbf{F} is the deformation gradient, T is the current absolute temperature, T_o is a reference absolute temperature, Ψ_o is the free energy at T_o , e_o is the internal energy at T_o , and \bar{c} is the heat capacity. Note that in what follows the heat capacity does not play a role and thus assuming it to be constant provides no restrictions on the presented theory.

In the special case where one has a separable free energy function for volumetric and deviatoric behavior then Eq. (1) is specialized to

$$\begin{aligned} \Psi(\mathbf{F}, T) = & \frac{T}{T_o} W_o(\bar{\mathbf{F}}) + \frac{T}{T_o} U_o(J) + \left(1 - \frac{T}{T_o}\right) e_o(J) \\ & + \bar{c} \left(T - T_o - T \ln \frac{T}{T_o}\right), \end{aligned} \quad (2)$$

where $J = \det[\mathbf{F}]$ is the Jacobian determinant, $\bar{\mathbf{F}} = J^{-1/3} \mathbf{F}$ is the volume preserving part of the deformation gradient, W_o is the deviatoric free energy at T_o , and U_o is the volumetric free energy at T_o .

3 Isotropic Thermoelasticity

As a particular example of the general setting outlined in Section 2, consider the case of a regularized neo-Hookean material. Appropriate choices for the functions in Eq. (2) are

$$W_o(\bar{\mathbf{F}}) = \frac{\mu}{2}(\bar{\mathbf{F}} : \bar{\mathbf{F}} - 3) \quad (3)$$

$$U_o(J) = \frac{\kappa}{4}(J^2 - 2\ln(J) - 1) \quad (4)$$

$$e_o(J) = 3\kappa\alpha T_o \ln(J), \quad (5)$$

where μ is the shear modulus, κ is the bulk modulus, and α is the coefficient of thermal expansion. Note that the above choices properly reduce to their small strain counterparts when the model is linearized about the reference configuration. The corresponding Cauchy stress tensor is given as

$$\boldsymbol{\sigma} = \frac{T}{T_o} \frac{\mu}{J} \text{dev}[\bar{\mathbf{b}}] + \left[\frac{T}{T_o} \frac{\kappa}{2} \left(J - \frac{1}{J} \right) + (T_o - T) 3\kappa\alpha \frac{1}{J} \right] \mathbf{1}, \quad (6)$$

where $\text{dev}[\cdot] = (\cdot) - \frac{1}{3}(\mathbf{1} : (\cdot))\mathbf{1}$, and $\bar{\mathbf{b}} = \bar{\mathbf{F}}\bar{\mathbf{F}}^T$. If we express Eq. (6) in terms of the inverse motion then one has

$$\boldsymbol{\sigma} = \frac{T}{T_o} \mu j \text{dev}[\bar{\mathbf{c}}^{-1}] + \left[\frac{T}{T_o} \frac{\kappa}{2} \left(\frac{1}{j} - j \right) + (T_o - T) 3\kappa\alpha j \right] \mathbf{1}, \quad (7)$$

where $j = 1/J$, $\mathbf{c} = \mathbf{f}^T \mathbf{f}$, and $\mathbf{f} = \mathbf{F}^{-1}$. For convenience split the stress as $\boldsymbol{\sigma} = \mathbf{s} + p\mathbf{1}$ so that the deviatoric stress

$$\mathbf{s} = \frac{T}{T_o} \mu j \text{dev}[\bar{\mathbf{c}}^{-1}] \quad (8)$$

and the pressure

$$p = \hat{p}(j) = \frac{T}{T_o} \frac{\kappa}{2} \left(\frac{1}{j} - j \right) + (T_o - T) 3\kappa\alpha j. \quad (9)$$

3.1 Inverse Three Field Finite Element Formulation

The three field formulation of Simo & Taylor (1991) is used in conjunction with the above model. Following from the appendix of Govindjee & Mihalic (1998), the Jacobian of the inverse motion and the pressure are introduced

as second and third field variables in the weak form. If the deformed body is denoted as \mathcal{S} with boundary $\partial\mathcal{S} = \overline{\partial\mathcal{S}_t} \cup \overline{\partial\mathcal{S}_\varphi}$ such that $\partial\mathcal{S}_t \cap \partial\mathcal{S}_\varphi = \emptyset$ and points in this configuration are denoted by \mathbf{x} , then the strong form equations for the three field inverse (penalized) incompressible problem are given by: for all $\mathbf{x} \in \mathcal{S}$

$$j = \theta, \quad (10)$$

$$p = \hat{p}(\theta), \quad (11)$$

and

$$\operatorname{div}[\mathbf{s} + p\mathbf{1}] + \hat{\mathbf{b}} = 0 \quad \text{and} \quad \boldsymbol{\sigma} = \boldsymbol{\sigma}^T; \quad (12)$$

for all $\mathbf{x} \in \partial\mathcal{S}_t$

$$\boldsymbol{\sigma}\mathbf{n} = \bar{\mathbf{t}}; \quad (13)$$

for all $\mathbf{x} \in \partial\mathcal{S}_\varphi$

$$\varphi = \bar{\varphi}, \quad (14)$$

with $\hat{\mathbf{b}}$, $\bar{\mathbf{t}}$ and $\bar{\varphi}$ as given data.

The corresponding weak form equations are given by

$$\tilde{G}_\theta(\varphi, \theta; \beta) = \int_{\mathcal{S}} [j - \theta]\beta = 0 \quad (15)$$

$$\tilde{G}_p(\theta, p; \alpha) = \int_{\mathcal{S}} [\hat{p}(\theta) - p]\alpha = 0, \quad (16)$$

and

$$\tilde{G}_\varphi(\varphi, p; \boldsymbol{\eta}) = \int_{\mathcal{S}} [\mathbf{s} : \operatorname{grad}(\boldsymbol{\eta}) + p \operatorname{div}(\boldsymbol{\eta})] + G_{ext} = 0 \quad (17)$$

where the first variations are such that $\boldsymbol{\eta} : \mathcal{S} \rightarrow \mathbb{R}^3$ and $\boldsymbol{\eta} = 0$ on $\partial\mathcal{S}_\varphi$, $\beta : \mathcal{S} \rightarrow \mathbb{R}$, $\alpha : \mathcal{S} \rightarrow \mathbb{R}$, and G_{ext} contains the contribution of the tractions $\bar{\mathbf{t}}$ and body forces $\hat{\mathbf{b}}$.

For the Q1/P0 approximation one assumes constant approximations per element for β , α , θ , and p . This results in explicit expressions on the element level for the mixed inverse Jacobian and pressure as:

$$\theta_e(\boldsymbol{\varphi}) = \frac{1}{v_e} \int_{\mathcal{S}_e} j \quad (18)$$

and

$$p_e(\boldsymbol{\varphi}) = \hat{p}(\theta_e), \quad (19)$$

where \mathcal{S}_e refers to an individual element domain and v_e is the ‘‘spatial element volume.’’ We can then substitute (19) back into (17) to arrive at a single weak form expression,

$$G(\boldsymbol{\varphi}; \boldsymbol{\eta}) = \tilde{G}_\varphi(\boldsymbol{\varphi}, p_e(\boldsymbol{\varphi}); \boldsymbol{\eta}) = 0. \quad (20)$$

Equation (20) represents a set of non-linear equations which can be solved for the inverse motion $\boldsymbol{\varphi}$.

The Newton-Raphson method can be applied to (20) to solve for the unknown motion. The needed tangent operator for using this technique in terms of an admissible second variation $\boldsymbol{\nu} : \mathcal{B} \rightarrow \mathbb{R}^3$ ($\boldsymbol{\nu} = 0$ on $\partial\mathcal{S}_\varphi$) is given by

$$\begin{aligned} D_1 G(\boldsymbol{\varphi}; \boldsymbol{\eta})[\boldsymbol{\nu}] &= \int_{\mathcal{S}_e} \text{sym}[\text{grad}(\boldsymbol{\eta})] : \left[2 \frac{\partial \mathbf{s}}{\partial \mathbf{c}} \right] : \text{sym}[\mathbf{f}^T \text{grad}(\boldsymbol{\nu})] \\ &+ \left(\int_{\mathcal{S}_e} \text{div}(\boldsymbol{\eta}) \right) \frac{d\hat{p}(\theta)/d\theta}{v_e} \left(\int_{\mathcal{B}_e} \text{DIV}(\boldsymbol{\nu}) \right). \end{aligned} \quad (21)$$

For the model at hand we have that

$$\frac{d\hat{p}}{d\theta}(\theta) = \frac{T}{T_o} \frac{\kappa}{2} \left(-\frac{1}{\theta^2} - 1 \right) + (T_o - T) 3\kappa\alpha. \quad (22)$$

And

$$\frac{\partial \mathbf{s}}{\partial \mathbf{c}} = \mu \frac{T}{T_o} j^{1/3} \left[\frac{5}{6} \text{dev} \bar{\mathbf{c}}^{-1} \otimes \bar{\mathbf{c}}^{-1} - \mathbb{I}_{\bar{\mathbf{c}}^{-1}} + \frac{1}{3} \mathbf{1} \otimes \bar{\mathbf{c}}^{-2} \right], \quad (23)$$

where $\bar{\mathbf{c}} = \bar{\mathbf{f}}^T \bar{\mathbf{f}}$, $\bar{\mathbf{f}} = j^{-1/3} \mathbf{f}$, and $[\mathbb{I}_{\bar{\mathbf{c}}^{-1}}]_{ijkl} = \frac{1}{2} (\bar{c}_{ik}^{-1} \bar{c}_{jl}^{-1} + \bar{c}_{il}^{-1} \bar{c}_{jk}^{-1})$.

The implementation of the model at this stage follows directly along the lines outlined in Govindjee & Mihalic (1998) for 2-D plane and 3-D continua.

4 Anisotropic Thermoelasticity

The general finite deformation model for orthotropic materials is given by Spencer (1984) in terms of two orthogonal material director vectors \mathbf{P} and \mathbf{Q} . In order to satisfy the requirement of objectivity the free energy density is given with respect to the Green-Lagrange strain tensor, \mathbf{E} . For orthotropy the free energy should be an isotropic function with respect to these three variables. Thus one can write

$$\Psi_o = \hat{\Psi}_o(I_1, I_2, I_3, I_4, I_5, I_6, I_7), \quad (24)$$

where the invariants can be defined as

$$I_1 = \text{tr}[\mathbf{E}] \quad (25)$$

$$I_2 = \mathbf{E} : \mathbf{E} \quad (26)$$

$$I_3 = \text{tr}[\mathbf{E}^3] \quad (27)$$

$$I_4 = \mathbf{P} \cdot \mathbf{E} \cdot \mathbf{P} \quad (28)$$

$$I_5 = \mathbf{P} \cdot \mathbf{E}^2 \cdot \mathbf{P} \quad (29)$$

$$I_6 = \mathbf{Q} \cdot \mathbf{E} \cdot \mathbf{Q} \quad (30)$$

$$I_7 = \mathbf{Q} \cdot \mathbf{E}^2 \cdot \mathbf{Q}. \quad (31)$$

$$(32)$$

Note that $\mathbf{P} \cdot \mathbf{Q} = 0$. In the special case of transverse isotropy the free energy function only depends on the first 5 invariants. In the case of modest strains but large displacements a practical version of the above model is one where one restricts attention to functions that are of most second order polynomials in the strain measure. This leads to the well known family of Saint-Venant Kirchhoff models.

4.1 Saint-Venant Kirchhoff Orthotropy

The basic expression for the Saint-Venant Kirchhoff model of orthotropy is given by

$$\begin{aligned} \Psi_o = & \frac{1}{2}\lambda I_1^2 + \mu I_2 + (\alpha_1 I_4 + \alpha_2 I_6) I_1 + 2\mu_1 I_5 + 2\mu_2 I_7 \\ & + \frac{1}{2}\beta_1 I_4^2 + \frac{1}{2}\beta_2 I_6^2 + \beta_3 I_4 I_6 \end{aligned} \quad (33)$$

The inclusion of thermal effects requires the specification of the internal energy. To allow for orthotropic thermal expansion there must be three coefficients of thermal expansion in the three orthotropic directions. An appropriate expression for the internal energy is given by

$$\begin{aligned}
e_o = & \alpha_p T_o [(\alpha_1 + \beta_1 + 2\mu + 4\mu_1)I_4 + (\alpha_2 + \beta_3)I_6 + (\lambda + \alpha_1)I_1] \\
& + \alpha_q T_o [(\alpha_2 + \beta_2 + 2\mu + 4\mu_2)I_6 + (\alpha_1 + \beta_3)I_4 + (\lambda + \alpha_2)I_1] \\
& + \alpha_* T_o [(\lambda + 2\mu)I_1 + (\alpha_1 - 2\mu)I_4 + (\alpha_2 - 2\mu)I_6]
\end{aligned} \tag{34}$$

The above constants are related to the entries in the 6×6 conventional stiffness matrix as follows when the \mathbf{P} and \mathbf{Q} directions line up with the 1- and 2-coordinate directions

$$\mathbf{C} = \begin{bmatrix} \lambda + 2\alpha_1 + \beta_1 + 2\mu + 4\mu_1 & \lambda + \alpha_1 + \alpha_2 + \beta_3 & \lambda + \alpha_1 & 0 & 0 & 0 \\ & \lambda + 2\alpha_2 + \beta_2 + 2\mu + 4\mu_2 & \lambda + \alpha_2 & 0 & 0 & 0 \\ & & \lambda + 2\mu & 0 & 0 & 0 \\ & & & \mu + \mu_1 + \mu_2 & 0 & 0 \\ & & & & \mu + \mu_2 & 0 \\ & & & & & \mu + \mu_1 \end{bmatrix} \tag{35}$$

This leads to the Cauchy stress being expressible as

$$\begin{aligned}
\boldsymbol{\sigma} = & j \left[\left(\lambda i_1 - \alpha_1 \frac{i_4}{\hat{i}_4} - \alpha_2 \frac{i_6}{\hat{i}_6} \right) \mathbf{c}^{-1} \right. \\
& + \left(\alpha_1 i_1 - \beta_1 \frac{i_4}{\hat{i}_4} - \beta_3 \frac{i_6}{\hat{i}_6} \right) \frac{1}{\hat{i}_4} \mathbf{p} \otimes \mathbf{p} + \left(\alpha_2 i_1 - \beta_2 \frac{i_6}{\hat{i}_6} - \beta_3 \frac{i_4}{\hat{i}_4} \right) \frac{1}{\hat{i}_6} \mathbf{q} \otimes \mathbf{q} \\
& + 2\mu \mathbf{c}^{-1} \boldsymbol{\varepsilon} + 2\mu_1 \frac{1}{\hat{i}_4} (\mathbf{p} \otimes \boldsymbol{\varepsilon} \mathbf{p} + \boldsymbol{\varepsilon} \mathbf{p} \otimes \mathbf{p}) + 2\mu_2 \frac{1}{\hat{i}_6} (\mathbf{q} \otimes \boldsymbol{\varepsilon} \mathbf{q} + \boldsymbol{\varepsilon} \mathbf{q} \otimes \mathbf{q}) \\
& + (T_o - T) \{ \alpha_p (\alpha_1 + \beta_1 + 2\mu + 4\mu_1) + \alpha_q (\alpha_1 + \beta_3) + \alpha_* (\alpha_1 - 2\mu) \} \frac{1}{\hat{i}_4} \mathbf{p} \otimes \mathbf{p} \\
& + (T_o - T) \{ \alpha_q (\alpha_2 + \beta_2 + 2\mu + 4\mu_2) + \alpha_p (\alpha_2 + \beta_3) + \alpha_* (\alpha_2 - 2\mu) \} \frac{1}{\hat{i}_6} \mathbf{q} \otimes \mathbf{q} \\
& \left. + (T_o - T) \{ \alpha_p (\lambda + \alpha_1) + \alpha_q (\lambda + \alpha_2) + \alpha_* (\lambda + 2\mu) \} \mathbf{c}^{-1} \right],
\end{aligned} \tag{36}$$

$$\tag{37}$$

where

$$i_1 = \text{tr}[\boldsymbol{\varepsilon}] \tag{38}$$

$$i_4 = (\mathbf{p} \otimes \mathbf{p}) : \mathbf{e} \quad i_6 = (\mathbf{q} \otimes \mathbf{q}) : \mathbf{e} \tag{39}$$

$$\hat{i}_4 = (\mathbf{p} \otimes \mathbf{p}) : \mathbf{c} \quad \hat{i}_6 = (\mathbf{q} \otimes \mathbf{q}) : \mathbf{c} \quad (40)$$

$$\boldsymbol{\varepsilon} = \frac{1}{2}(\mathbf{c}^{-1} - \mathbf{1}) \quad \mathbf{e} = \frac{1}{2}(\mathbf{c} - \mathbf{1}) \quad (41)$$

$$\mathbf{P} = \frac{\mathbf{f}\mathbf{q}}{\|\mathbf{f}\mathbf{p}\|} \quad \mathbf{Q} = \frac{\mathbf{f}\mathbf{q}}{\|\mathbf{f}\mathbf{q}\|} \quad (42)$$

4.2 Saint-Venant Kirchhoff Transverse Isotropy

The case of transverse isotropy can be recovered as a sub-case of orthotropy. If the transverse direction is associated with \mathbf{P} then we can set $\alpha_2 = \mu_2 = \beta_2 = \beta_3 = 0$ and $\alpha_q = \alpha_*$ in the previous section to recover a model appropriate for transverse isotropy. No other changes are required.

4.3 Tangent Operator

The inverse tangent operator is determined for this model within the context of the displacement formulation of Govindjee & Mihalic (1996). Thus one needs to determine the derivatives $\partial\boldsymbol{\sigma}/\partial\mathbf{c}$. Thus it is useful to note that

$$\frac{\partial \hat{i}_1}{\partial \mathbf{c}} = -\frac{1}{2}\mathbf{c}^{-2} \quad (43)$$

$$\frac{\partial}{\partial \mathbf{c}} \left(\frac{1}{\hat{i}_4} \right) = -\frac{\mathbf{p} \otimes \mathbf{p}}{\hat{i}_4^2} \quad (44)$$

$$\frac{\partial}{\partial \mathbf{c}} \left(-\frac{\hat{i}_4}{\hat{i}_4} \right) = -\frac{1}{2} \frac{\mathbf{p} \otimes \mathbf{p}}{\hat{i}_4^2} \quad (45)$$

$$\frac{\partial}{\partial \mathbf{c}} \left(\frac{1}{\hat{i}_6} \right) = -\frac{\mathbf{q} \otimes \mathbf{q}}{\hat{i}_6^2} \quad (46)$$

$$\frac{\partial}{\partial \mathbf{c}} \left(-\frac{\hat{i}_6}{\hat{i}_6} \right) = -\frac{1}{2} \frac{\mathbf{q} \otimes \mathbf{q}}{\hat{i}_6^2} \quad (47)$$

$$\frac{\partial \mathbf{c}^{-1}}{\partial \mathbf{c}} = -\frac{1}{2}\mathbb{I}\mathbf{c}^{-1} \quad (48)$$

$$\frac{\partial \mathbf{c}^{-2}}{\partial \mathbf{c}} = -\text{sym}(\mathbf{c}^{-1}, \mathbf{c}^{-2}) \quad (49)$$

$$\text{sym}(\mathbf{A}, \mathbf{B})_{ijkl} = \frac{1}{2} [A_{ik}B_{jl} + A_{il}B_{jk} + B_{ik}A_{jl} + B_{il}A_{jk}] \quad (50)$$

$$\frac{\partial}{\partial \mathbf{c}} (\mathbf{p} \otimes \boldsymbol{\varepsilon}\mathbf{p} + \boldsymbol{\varepsilon}\mathbf{p} \otimes \mathbf{p}) = -\frac{1}{2}\text{sym}(\mathbf{p}, \mathbb{I}\mathbf{c}^{-1}, \mathbf{p}) \quad (51)$$

$$\text{sym}(\mathbf{a}, \mathbb{B}, \mathbf{a})_{ijkl} = a_i\mathbb{B}_{jmkl}a_m + a_j\mathbb{B}_{imkl}a_m \quad (52)$$

With these expressions it is possible to construct the tangent for the Saint-Venant Kirchhoff models presented above as:

$$\begin{aligned}
\frac{\partial \boldsymbol{\sigma}}{\partial \mathbf{c}} &= \frac{1}{2} \boldsymbol{\sigma} \otimes \mathbf{c}^{-1} + j \frac{T}{T_o} \left\{ - \left(\lambda i_1 - \alpha_1 \frac{i_4}{\hat{i}_4} - \alpha_2 \frac{i_6}{\hat{i}_6} - \mu \right) \mathbb{I}_{\mathbf{c}^{-1}} \right. \\
&\quad - \frac{1}{2} \mathbf{c}^{-1} \otimes \left(\lambda \mathbf{c}^{-2} + \frac{\alpha_1}{\hat{i}_4^2} \mathbf{p} \otimes \mathbf{p} + \frac{\alpha_2}{\hat{i}_6^2} \mathbf{q} \otimes \mathbf{q} \right) \\
&\quad - \left(\alpha_1 i_1 - \beta_1 \frac{i_4}{\hat{i}_4} - \beta_3 \frac{i_6}{\hat{i}_6} \right) \frac{1}{\hat{i}_4^2} \mathbf{p} \otimes \mathbf{p} \otimes \mathbf{p} \otimes \mathbf{p} \\
&\quad - \frac{1}{2} \frac{1}{\hat{i}_4} \mathbf{p} \otimes \mathbf{p} \otimes \left(\alpha_1 \mathbf{c}^{-2} + \frac{\beta_1}{\hat{i}_4^2} \mathbf{p} \otimes \mathbf{p} + \frac{\beta_3}{\hat{i}_6^2} \mathbf{q} \otimes \mathbf{q} \right) \\
&\quad - \left(\alpha_2 i_1 - \beta_2 \frac{i_6}{\hat{i}_6} - \beta_3 \frac{i_4}{\hat{i}_4} \right) \frac{1}{\hat{i}_6^2} \mathbf{q} \otimes \mathbf{q} \otimes \mathbf{q} \otimes \mathbf{q} \\
&\quad - \frac{1}{2} \frac{1}{\hat{i}_6} \mathbf{q} \otimes \mathbf{q} \otimes \left(\alpha_2 \mathbf{c}^{-2} + \frac{\beta_2}{\hat{i}_6^2} \mathbf{q} \otimes \mathbf{q} + \frac{\beta_3}{\hat{i}_4^2} \mathbf{p} \otimes \mathbf{p} \right) \\
&\quad - \mu \text{sym}(\mathbf{c}^{-1}, \mathbf{c}^{-2}) \\
&\quad - \frac{2\mu_1}{\hat{i}_4^2} [\mathbf{p} \otimes \boldsymbol{\varepsilon} \mathbf{p} + \boldsymbol{\varepsilon} \mathbf{p} \otimes \mathbf{p}] \otimes \mathbf{p} \otimes \mathbf{p} \\
&\quad - \mu_1 \frac{1}{\hat{i}_4} \text{sym}(\mathbf{p}, \mathbb{I}_{\mathbf{c}^{-1}}, \mathbf{p}) \\
&\quad - \frac{2\mu_2}{\hat{i}_6^2} [\mathbf{q} \otimes \boldsymbol{\varepsilon} \mathbf{q} + \boldsymbol{\varepsilon} \mathbf{q} \otimes \mathbf{q}] \otimes \mathbf{q} \otimes \mathbf{q} \\
&\quad - \mu_2 \frac{1}{\hat{i}_6} \text{sym}(\mathbf{q}, \mathbb{I}_{\mathbf{c}^{-1}}, \mathbf{q}) \left. \right\} \\
&\quad - j(T_o - T) \left\{ \right. \\
&\quad \quad (\alpha_p(\alpha_1 + \beta_1 + 2\mu + 4\mu_1) + \alpha_q(\alpha_1 + \beta_3) + \alpha_*(\alpha_1 - 2\mu)) \frac{1}{\hat{i}_4^2} \mathbf{p} \otimes \mathbf{p} \otimes \mathbf{p} \otimes \mathbf{p} \\
&\quad \quad + (\alpha_q(\alpha_2 + \beta_2 + 2\mu + 4\mu_2) + \alpha_p(\alpha_2 + \beta_3) + \alpha_*(\alpha_2 - 2\mu)) \frac{1}{\hat{i}_6^2} \mathbf{q} \otimes \mathbf{q} \otimes \mathbf{q} \otimes \mathbf{q} \\
&\quad \quad + \frac{1}{2} (\alpha_p(\lambda + \alpha_1) + \alpha_q(\lambda + \alpha_2) + \alpha_*(\lambda + 2\mu)) \mathbb{I}_{\mathbf{c}^{-1}} \left. \right\} \\
&\quad + \frac{\partial \boldsymbol{\sigma}}{\partial \mathbf{q}} \frac{\partial \mathbf{q}}{\partial \mathbf{c}}.
\end{aligned} \tag{53}$$

In the above, it is assumed that the mapped orthotropic direction \mathbf{p} is part of the given data. Note that the last term arises because once \mathbf{p} has been specified \mathbf{q} is given in terms of the unknown motion as

$$\mathbf{q} = \frac{\mathbf{f}^{-1} \mathbf{T} \mathbf{f} \mathbf{p}}{\|\mathbf{f}^{-1} \mathbf{T} \mathbf{f} \mathbf{p}\|}, \tag{54}$$

where

$$\mathbf{T} \rightarrow \begin{bmatrix} 0 & -1 & 0 \\ 1 & 0 & 0 \\ 0 & 0 & 1 \end{bmatrix} \quad (55)$$

To compute the remaining derivatives one needs to note the polar decomposition $\mathbf{f} = r\mathbf{u}$ and that

$$\frac{\partial \mathbf{f}}{\partial \mathbf{c}} = \frac{\partial \mathbf{f}}{\partial \mathbf{u}} : \frac{\partial \mathbf{u}}{\partial \mathbf{c}}. \quad (56)$$

The necessary information is completed by noticing that

$$\left(\frac{\partial \mathbf{f}}{\partial \mathbf{u}} \right)_{Aijk} = r_{Ai} \mathbb{I}_{lijk} \quad (57)$$

and

$$\begin{aligned} \frac{\partial \mathbf{u}}{\partial \mathbf{c}} = & \sum_i \frac{1}{2\lambda_i} \mathbf{n}_i \otimes \mathbf{n}_i \otimes \mathbf{n}_i \otimes \mathbf{n}_i \\ & + \frac{1}{2} \sum_{i \neq j} \frac{1}{\lambda_i + \lambda_j} (\mathbf{n}_i \otimes \mathbf{n}_j \otimes \mathbf{n}_i \otimes \mathbf{n}_j + \mathbf{n}_i \otimes \mathbf{n}_j \otimes \mathbf{n}_j \otimes \mathbf{n}_i), \end{aligned} \quad (58)$$

where λ_i and \mathbf{n}_i are the eigenvalues and eigenvectors of \mathbf{u} .

5 Axis-Symmetry

The implementation of the above models for axis-symmetry requires several modifications to a plane inverse element. The following steps are involved in the conversion.

First, regard the 1- and 2-directions as r and z respectively. Let the 3-direction be the angular coordinate θ . While this results in a left-handed coordinate system, it poses no real issues of note for the purposes at hand. With this

ordering the deformation gradient

$$\mathbf{f} \rightarrow \begin{bmatrix} f_{Rr} & f_{Rz} & 0 \\ f_{Zr} & f_{Zz} & 0 \\ 0 & 0 & \frac{R}{r} \end{bmatrix}, \quad (59)$$

where the components are computed in the usual manner (e.g. $f_{Zr} = \partial\varphi_Z/\partial x_r$). Lower case letters refer to the spatial configuration and upper case letters refer to the reference configuration. At the Gauss Point level the stresses are computed using \mathbf{f} as shown above with the usual Cartesian component formulas. This results in the reporting of the mixed covariant-contravariant stress components. These are the “standard” components and permit one to avoid explicitly considering the non-constant metric tensor that appears when using curvilinear coordinates. The ordering of the tangent matrix is conveniently taken as

$$\mathbf{D} \rightarrow \begin{bmatrix} D_{rrrr} & D_{rrzz} & D_{rr\theta\theta} & D_{rrrz} \\ & D_{zzzz} & D_{zz\theta\theta} & D_{zzrz} \\ & & D_{\theta\theta\theta\theta} & D_{\theta\theta rz} \\ \text{sym.} & & & D_{rzrz} \end{bmatrix}. \quad (60)$$

At the element level several changes are needed in order to account for the fact that radial displacements produce hoop strains; i.e., that $[\text{grad}(\mathbf{u})]_{\theta\theta} = u_r/r$. This is most easily effected by inserting an extra row in the usual strain-displacement matrix. Thus,

$$\mathbf{B}^A = \begin{bmatrix} N_{,r}^A & 0 \\ 0 & N_{,z}^A \\ \frac{N^A}{r} & 0 \\ N_{,z}^A & N_{,r}^A \end{bmatrix} \quad (61)$$

The right-hand-side may then be computed as $\mathbf{B}^T \boldsymbol{\sigma}$, where the stress is taken

in vector form as

$$\boldsymbol{\sigma} = \begin{pmatrix} \sigma_{rr} \\ \sigma_{zz} \\ \sigma_{\theta\theta} \\ \sigma_{rz} \end{pmatrix} \quad (62)$$

and $\mathbf{B} = [\mathbf{B}^1, \mathbf{B}^2, \dots, \mathbf{B}^{nen}]$

When computing the divergence terms for the mixed contributions to the tangent one should note that

$$\text{div}(\boldsymbol{\eta}) = \sum_A \eta_r^A (N_{,r}^A + \frac{N^A}{r}) + \eta_z^A N_{,z}^A \quad (63)$$

$$\text{DIV}(\boldsymbol{\nu}) = \sum_A \nu_R^A (N_{,R}^A + \frac{N^A}{R}) + \nu_Z^A N_{,Z}^A \quad (64)$$

Note that the spatial integration volume is taken as $r dr 1 dz$; i.e. a one radian sector is assumed for the angular integration. The reference integration volume is given by $jr dr 1 dz$.

For inverse elements one must also account for the \mathbf{f}^T modification to the symmetric gradient to the second variation $\boldsymbol{\nu}$. This is most easily effected by using $\mathbf{B}^T \widehat{\mathbf{D}} \mathbf{B}$ for the integrand in the first integral of Eq. (21), where

$$\widehat{\mathbf{B}}^A = \begin{bmatrix} N_{,r}^A f_{rr} & N_{,r}^A f_{zr} \\ N_{,z}^A f_{rz} & N_{,z}^A f_{zz} \\ \frac{N^A}{r} f_{\theta\theta} & 0 \\ N_{,z}^A f_{rr} + N_{,r}^A f_{rz} & N_{,z}^A f_{zr} + N_{,r}^A f_{zz} \end{bmatrix} \quad (65)$$

and $\widehat{\mathbf{B}} = [\widehat{\mathbf{B}}^1, \widehat{\mathbf{B}}^2, \dots, \widehat{\mathbf{B}}^{nen}]$. Note that this modification eliminates the need for the block diagonal matrix of \mathbf{f}^T 's that appears in the original papers by Govindjee & Mihalic (1996) and Govindjee & Mihalic (1998). By combining this block diagonal matrix with the strain-displacement operator one can more easily preserve the traditional structure of the element stiffness construction.

Table 1

Cook's plane strain panel with temperature change. Global residual norms.

Iteration	Residual Norm	Relative Residual Norm
1	2.4606275E+00	1.0000000E+00
2	7.2575605E+05	2.9494756E+05
3	5.4541417E+01	2.2165654E+01
4	1.0909316E-02	4.4335506E-03
5	2.3363872E-06	9.4950870E-07

6 Examples

To document the behavior of the outlined formulation several simple examples are considered in the next few sections.

6.1 Cook's Plane Strain Panel with Temperature Change

As a first example consider a neo-Hookean Cook's Panel where $\kappa = 10^8$ and $\mu = 80.1938$. The temperature in the deformed configuration is taken as $T = 270$ and the temperature in the "to-be-manufactured" configuration is $T_o = 300$. The coefficient of thermal expansion is 10^{-6} . Fig. 1 shows the initial deformed and cooled shape with the loads upon it. Also shown is the computed heated inverse motion. The correct answer corresponds to the skew geometry of Cook's panel which is straight sided. As can be seen from the figure a straight sided panel has been recovered. The tip displacement matches a forward computation on the same problem to all digits. The undeformed reference geometry is that shown in Govindjee & Mihalic (1998).

The problem was solved using 10 inverse load steps each of which took 5 global newton iterations. The convergence of the global residual norm was asymptotically quadratic as is shown in Table 1 for a typical load step. The residual reduction shown corresponds to relative reduction in the energy norm of 21 orders of magnitude.

6.2 Axis-Symmetric cap

In this example we consider an axis-symmetric cap (with a pin-hole on the central axis). The cap is neo-hookean; $\kappa = 10^4$ and $\mu = 10^2$. In the deformed state the cap is under an internal pressure of 2. The inner radius of the cap is 2.25 and the outer radius is 3.0. The top wall ranges from $z = 1$ to $z = 1.5$.

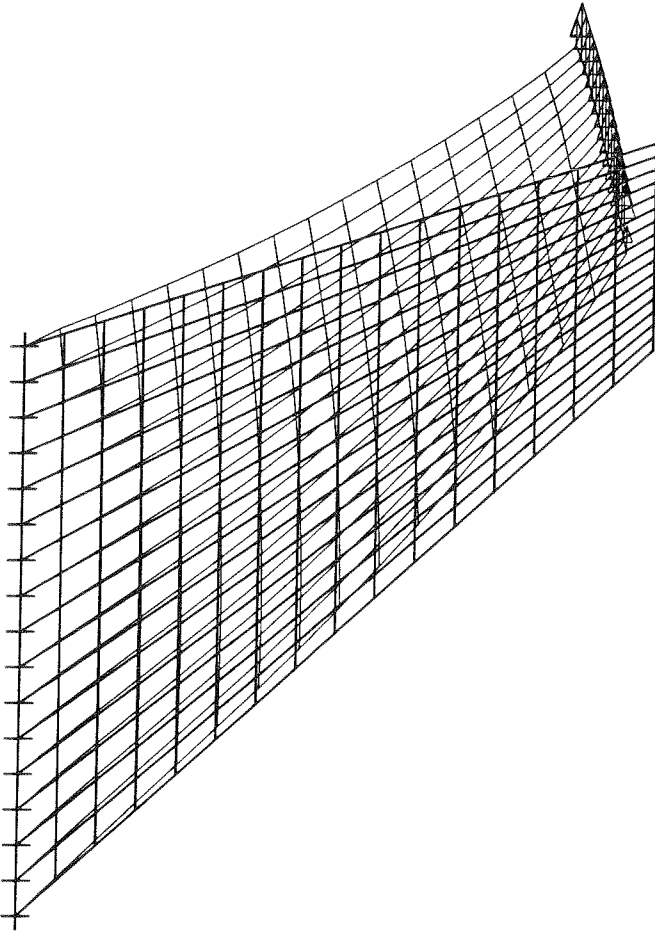


Fig. 1. Cook's plane strain panel with temperature change. Initial geometry (light-line) and computed inverse geometry (heavy-line).

The lower edge of the sidewall is set on roller. The unloaded configuration is to be computed. Shown in Fig. 2 is the initial deformed state and the computed undeformed state. The computation was checked by performing a forward computation on the predicted undeformed state and was found to be accurate to all digits.

The problem was solved using 2 inverse load steps each of which took 5 global newton iterations. The convergence of the global residual norm was asymptotically quadratic as is shown in Table 2 for the first load step.

6.3 *Axis-Symmetric Transverse Isotropy with Temperature Change*

In this example we consider the axis-symmetric geometry show in Fig. 3. The system is composed of an isotropic neo-hookean inner band with $\kappa = 10^4$, $\mu = 80$, and $\alpha = 2 \times 10^{-6}$. The ribs are transverse isotropic with $C_{11} =$

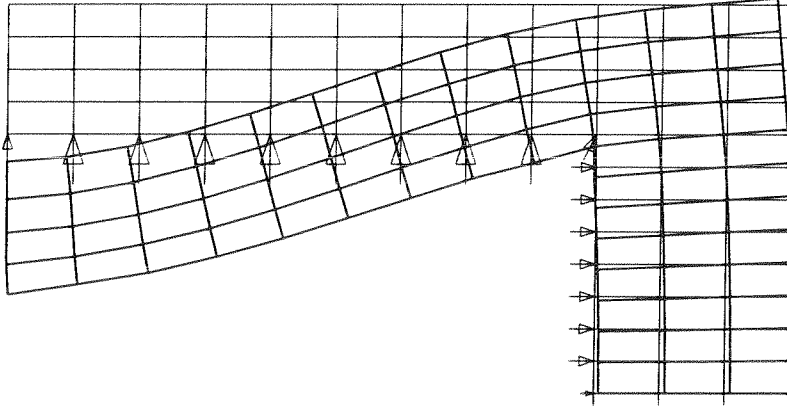


Fig. 2. Axis-Symmetric cap with pin-hole. Initial geometry (light-line) with load and computed inverse geometry (heavy-line).

Table 2

Axis-Symmetric cap with pin-hole: Global residual norms.

Iteration	Residual Norm	Relative Residual Norm
1	8.0525617E-01	1.0000000E+00
2	2.1691048E+02	2.6936829E+02
3	7.2898256E-01	9.0528032E-01
4	1.6396355E-05	2.0361663E-05
5	7.8812905E-12	9.7873084E-12

12110, $C_{22} = 10200$, $C_{12} = 10100$, $C_{23} = 10000$, $C_{44} = 500$, $\alpha_p = 1 \times 10^{-6}$ and $\alpha_q = \alpha_* = 1.5 \times 10^{-6}$. The angle of the spatial director \mathbf{p} for the plane of transverse isotropy is taken as 0.0 rad with respect to the radial (horizontal) direction for the bottom rib and as 1.5 rad for the top rib.

In the deformed state, the temperature is $T = 270$ and the inner surface is subject to an inflation pressure of 25. The undeformed configuration is at a temperature of $T_o = 350$. Fig. 3 shows the computed undeformed (hot) geometry. For the specification of the geometry used see Appendix C.

The computation was executed in a single time step with 7 iterations. The convergence was quadratic as shown in Table 3. The answer (as checked against a forward solution) was correct to all significant digits.

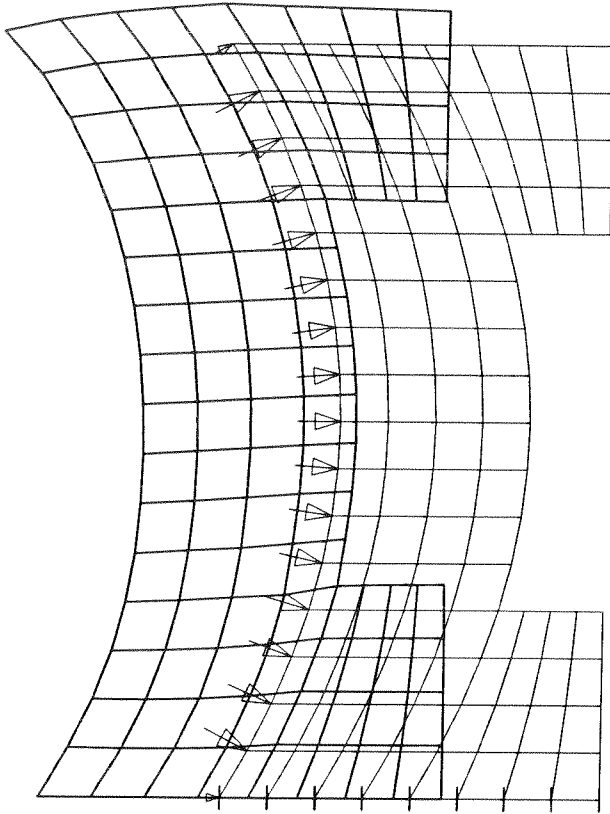


Fig. 3. Axis-Symmetric Bi-Material Band. Initial geometry (light-line) with load and computed inverse geometry (heavy-line).

Table 3

Axis-Symmetric Bi-Material Band: Energy norms.

Iteration	Energy Norm	Relative Energy Norm
1	-3.217522165840916E+01	1.000000000000000E+00
2	-7.665454629867564E+01	2.382409268613122E+00
3	-5.116391766639881E-01	1.590165196360873E-02
4	-3.053214350661301E-03	9.489334317805166E-05
5	-1.283754804282023E-07	3.989886434695338E-09
6	-8.387627255489300E-15	2.606859198838542E-16
7	-9.529547438470103E-21	2.961765901612525E-22

6.4 Axis-Symmetric Orthotropy with Temperature Change

In this example we consider the same problem as in the previous example however the ribs are now taken as orthotropic. Their properties are taken as $C_{11} = 12110$, $C_{22} = 10200$, $C_{33} = 10300$, $C_{12} = 10100$, $C_{23} = 10000$, $C_{13} =$

Table 4

Axis-Symmetric Bi-Material Band Orthotropic Case: Residual norms.

Iteration	Residual Norm	Relative Residual Norm
1	2.3114523E+01	1.0000000E+00
2	1.0464814E+03	4.5273761E+01
3	1.7596354E+01	7.6126833E-01
4	1.0889067E+01	4.7109202E-01
5	8.3921940E-02	3.6307018E-03
6	1.0668298E-02	4.6154090E-04
7	1.9096628E-03	8.2617443E-05
8	3.4370858E-04	1.4869811E-05
9	6.2657260E-05	2.7107313E-06
10	1.1516999E-05	4.9825812E-07
11	2.1304459E-06	9.2169149E-08
12	3.9595014E-07	1.7129929E-08

10500, $C_{44} = 500$, $C_{55} = 300$, $C_{66} = 400$, $\alpha_p = 1 \times 10^{-6}$, $\alpha_q = 1.5 \times 10^{-6}$ and $\alpha_* = 2 \times 10^{-6}$. The angle of the spatial director \mathbf{p} for the first orthotropic direction is taken as 0.0 rad with respect to the radial (horizontal) direction for the bottom rib and as 1.5 rad for the top rib. In the deformed state, the temperature is $T = 270$ and the inner surface is again subject to an inflation pressure of 25. The undeformed configuration is at a temperature of $T_o = 350$. The input deck is shown in Appendix D.

The computation was executed in a single time step with 12 iterations. The tangent expression used does not include the last term in Eq. (53) and thus leads to linear convergence of the problem. The convergence of the residual norm is shown in Table 4. Even though the tangent is not complete this large deformation problem converges in a single load step with only a few more iterations than were required in the previous example. The answer (as checked against a forward solution) was correct to all significant digits.

References

- Chadwick, P. (1974). Thermo-mechanics of rubberlike materials, *Philosophical Transactions of the Royal Society of London Series A* **276**: 371–403.
- Euler, L. (1744). Methodus inveniendi lineas curvas, = *Opera omnia I* **24**: 264–266. (1952).

- Govindjee, S. & Mihalic, P. (1996). Computational methods for inverse finite elastostatics, *Computer Methods in Applied Mechanics and Engineering* **136**: 47–57.
- Govindjee, S. & Mihalic, P. (1998). Computational methods for inverse deformations in quasi-incompressible finite elasticity, *International Journal for Numerical Methods in Engineering* **43**: 821–828.
- Simo, J. & Taylor, R. (1991). Quasi-incompressible finite elasticity in principal stretches. Continuum basis and numerical algorithms, *Computer Methods in Applied Mechanics and Engineering* **85**: 273–310.
- Spencer, A. (1984). Constitutive theory for strongly anisotropic solids, in A. Spencer (ed.), *Continuum Theory of the Mechanics of Fibre-Reinforced Composites*, Springer-Verlag, Wien, pp. 1–32.

A Input file for Example 6.1

feap * Cook Membrane Problem
0,0,0,2,2,4

COORDinates

```

1 0 0.0000000E+00 0.0000000E+00
2 0 3.0015015E+00 2.9692679E+00
3 0 6.0061653E+00 5.9232720E+00
4 0 9.0228606E+00 8.8624084E+00
5 0 1.2067409E+01 1.1797020E+01
6 0 1.5135184E+01 1.4750480E+01
7 0 1.8216885E+01 1.7748294E+01
8 0 2.1288545E+01 2.0808989E+01
9 0 2.4331741E+01 2.3944699E+01
10 0 2.7322395E+01 2.7158373E+01
11 0 3.0248091E+01 3.0449451E+01
12 0 3.3093391E+01 3.3813163E+01
13 0 3.5852993E+01 3.7246368E+01
14 0 3.8515264E+01 4.0742714E+01
15 0 4.1075796E+01 4.4298812E+01
16 0 4.3517106E+01 4.7896257E+01
17 0 4.5828610E+01 5.1504078E+01
18 0 0.0000000E+00 2.7500000E+00
19 0 3.0011375E+00 5.6066311E+00
20 0 6.0116143E+00 8.4491504E+00
21 0 9.0466112E+00 1.1274670E+01
22 0 1.2106110E+01 1.4096866E+01
23 0 1.5183864E+01 1.6941324E+01
24 0 1.8258945E+01 1.9831263E+01
25 0 2.1315134E+01 2.2786052E+01
26 0 2.4329386E+01 2.5814689E+01
27 0 2.7289021E+01 2.8921108E+01
28 0 3.0178504E+01 3.2102398E+01
29 0 3.2991764E+01 3.5356056E+01
30 0 3.5718946E+01 3.8676579E+01
31 0 3.8354449E+01 4.2061412E+01
32 0 4.0889431E+01 4.5502057E+01
33 0 4.3304447E+01 4.8987183E+01
34 0 4.5610738E+01 5.2490630E+01
35 0 0.0000000E+00 5.5000000E+00
36 0 3.0032641E+00 8.2447498E+00
37 0 6.0245453E+00 1.0969059E+01
38 0 9.0711360E+00 1.3675018E+01
39 0 1.2141924E+01 1.6384255E+01
40 0 1.5218087E+01 1.9119682E+01
41 0 1.8284468E+01 2.1905602E+01
42 0 2.1318028E+01 2.4756425E+01
43 0 2.4305679E+01 2.7681436E+01
44 0 2.7231519E+01 3.0681204E+01
45 0 3.0089211E+01 3.3754594E+01
46 0 3.2869822E+01 3.6897645E+01
47 0 3.5568558E+01 4.0107052E+01
48 0 3.8178431E+01 4.3379838E+01
49 0 4.0688719E+01 4.6706817E+01
50 0 4.3086005E+01 5.0086888E+01
51 0 4.5399087E+01 5.3487646E+01
52 0 0.0000000E+00 8.2500000E+00
53 0 3.0079792E+00 1.0878970E+01
54 0 6.0371189E+00 1.3478314E+01
55 0 9.0951942E+00 1.6065239E+01
56 0 1.2167383E+01 1.8660513E+01
57 0 1.5240090E+01 2.1290698E+01
58 0 1.8289298E+01 2.3973822E+01
59 0 2.1300962E+01 2.6724081E+01
60 0 2.4257704E+01 2.9545989E+01
61 0 2.7153034E+01 3.2440691E+01
62 0 2.9977919E+01 3.5406089E+01
63 0 3.2729608E+01 3.8438955E+01
64 0 3.5400854E+01 4.1538176E+01
65 0 3.7987855E+01 4.4697949E+01
66 0 4.0475319E+01 4.7916906E+01
67 0 4.2867368E+01 5.1192729E+01
68 0 4.5187715E+01 5.4491304E+01
69 0 0.0000000E+00 1.1000000E+01
70 0 3.0109769E+00 1.3504637E+01
71 0 6.0504394E+00 1.5979189E+01
72 0 9.1116969E+00 1.8445038E+01
73 0 1.2184738E+01 2.0930733E+01
74 0 1.5244840E+01 2.3456457E+01
75 0 1.8276785E+01 2.6040449E+01
76 0 2.1260422E+01 2.8690579E+01
77 0 2.4188506E+01 3.1410661E+01
78 0 2.7050964E+01 3.4200332E+01
79 0 2.9846934E+01 3.7057363E+01
80 0 3.2569446E+01 3.9981302E+01
81 0 3.5217789E+01 4.2968863E+01
82 0 3.7781254E+01 4.6018923E+01
83 0 4.0255091E+01 4.9131041E+01

```

```

84 0 4.2646398E+01 5.2303792E+01
85 0 4.4976267E+01 5.5497873E+01
86 0 0.0000000E+00 1.3750000E+01
87 0 3.0154242E+00 1.6124711E+01
88 0 6.0582465E+00 1.8470223E+01
89 0 9.1238577E+00 2.0819774E+01
90 0 1.2188273E+01 2.3196313E+01
91 0 1.5235735E+01 2.5622016E+01
92 0 1.8242443E+01 2.8107361E+01
93 0 2.1199487E+01 3.0658680E+01
94 0 2.4094608E+01 3.3276773E+01
95 0 2.6928126E+01 3.5960513E+01
96 0 2.9693570E+01 3.8710098E+01
97 0 3.2392327E+01 4.1523525E+01
98 0 3.5016614E+01 4.4401541E+01
99 0 3.7563309E+01 4.7341819E+01
100 0 4.0027166E+01 5.0349994E+01
101 0 4.2424836E+01 5.3415854E+01
102 0 4.4759644E+01 5.6508221E+01
103 0 0.0000000E+00 1.6500000E+01
104 0 3.0163472E+00 1.8737111E+01
105 0 6.0651899E+00 2.0957260E+01
106 0 9.1254875E+00 2.3189986E+01
107 0 1.2182038E+01 2.5462950E+01
108 0 1.5207171E+01 2.7789345E+01
109 0 1.8189565E+01 3.0178018E+01
110 0 2.1113386E+01 3.2630104E+01
111 0 2.3979268E+01 3.5144949E+01
112 0 2.6780747E+01 3.7723072E+01
113 0 2.9521445E+01 4.0363208E+01
114 0 3.2194906E+01 4.3067907E+01
115 0 3.4801346E+01 4.5834736E+01
116 0 3.7332469E+01 4.8668878E+01
117 0 3.9795305E+01 5.1569420E+01
118 0 4.2197701E+01 5.4529990E+01
119 0 4.4539694E+01 5.7518665E+01
120 0 0.0000000E+00 1.9250000E+01
121 0 3.0191028E+00 2.1347518E+01
122 0 6.0646827E+00 2.3439681E+01
123 0 9.1218497E+00 2.5562146E+01
124 0 1.2159328E+01 2.7732438E+01
125 0 1.5162959E+01 2.9962904E+01
126 0 1.8111764E+01 3.2254463E+01
127 0 2.1005703E+01 3.4605961E+01
128 0 2.3837397E+01 3.7017153E+01
129 0 2.6612917E+01 3.9486914E+01
130 0 2.9326546E+01 4.2019221E+01
131 0 3.1981269E+01 4.4612325E+01
132 0 3.4569195E+01 4.7271546E+01
133 0 3.7093374E+01 4.9996022E+01
134 0 3.9555211E+01 5.2790789E+01
135 0 4.1967084E+01 5.5641655E+01
136 0 4.4311131E+01 5.8531539E+01
137 0 0.0000000E+00 2.2000000E+01
138 0 3.0172126E+00 2.3953907E+01
139 0 6.0634789E+00 2.5924618E+01
140 0 9.1051764E+00 2.7937434E+01
141 0 1.2124940E+01 3.0010545E+01
142 0 1.5094857E+01 3.2145074E+01
143 0 1.8012936E+01 3.4338608E+01
144 0 2.0869571E+01 3.6588399E+01
145 0 2.3673539E+01 3.8892202E+01
146 0 2.6419649E+01 4.1254948E+01
147 0 2.9113377E+01 4.3675447E+01
148 0 3.1747562E+01 4.6160455E+01
149 0 3.4324939E+01 4.8707918E+01
150 0 3.6842075E+01 5.1325733E+01
151 0 3.9309753E+01 5.4008714E+01
152 0 4.1727167E+01 5.6753543E+01
153 0 4.4076971E+01 5.9542197E+01
154 0 0.0000000E+00 2.4750000E+01
155 0 3.0180858E+00 2.6563014E+01
156 0 6.0527654E+00 2.8411850E+01
157 0 9.0818661E+00 3.0323081E+01
158 0 1.2068629E+01 3.2299970E+01
159 0 1.5007227E+01 3.4339057E+01
160 0 1.7883723E+01 3.6432941E+01
161 0 2.0709994E+01 3.8576073E+01
162 0 2.3481313E+01 4.0773458E+01
163 0 2.6205989E+01 4.3023836E+01
164 0 2.8877231E+01 4.5336270E+01
165 0 3.1498509E+01 4.7707805E+01
166 0 3.4064527E+01 5.0147624E+01
167 0 3.6582090E+01 5.2652121E+01
168 0 3.9053121E+01 5.526271E+01
169 0 4.1480624E+01 5.7860251E+01
170 0 4.3831691E+01 6.053955E+01
171 0 0.0000000E+00 2.7500000E+01
172 0 3.0126707E+00 2.9172481E+01
173 0 6.0411135E+00 3.0909808E+01
174 0 9.0396504E+00 3.2721771E+01
175 0 1.1995684E+01 3.4605928E+01

```

176	0	1.4887236E+01	3.6548063E+01	268	0	3.2162059E+01	5.8753864E+01
177	0	1.7729591E+01	3.8535949E+01	269	0	3.4702218E+01	6.0553707E+01
178	0	2.0518531E+01	4.0572941E+01	270	0	3.7218869E+01	6.2419551E+01
179	0	2.3266421E+01	4.2656555E+01	271	0	3.9704739E+01	6.4373716E+01
180	0	2.5966440E+01	4.4799058E+01	272	0	4.2091494E+01	6.6516792E+01
181	0	2.8622757E+01	4.6996267E+01	273	0	0.0000000E+00	4.4000000E+01
182	0	3.1229869E+01	4.9259558E+01	274	0	2.6533442E+00	4.5400071E+01
183	0	3.3791614E+01	5.1584343E+01	275	0	5.2936393E+00	4.6455241E+01
184	0	3.6308134E+01	5.3979126E+01	276	0	8.0354679E+00	4.7663546E+01
185	0	3.8787637E+01	5.6437383E+01	277	0	1.0719725E+01	4.8840361E+01
186	0	4.1221630E+01	5.8965308E+01	278	0	1.3425061E+01	5.0091419E+01
187	0	4.3578357E+01	6.1561333E+01	279	0	1.6095240E+01	5.1367093E+01
188	0	0.0000000E+00	3.0250000E+01	280	0	1.8761213E+01	5.2702107E+01
189	0	3.0110370E+00	3.1790482E+01	281	0	2.1398917E+01	5.4080855E+01
190	0	6.0145067E+00	3.3420042E+01	282	0	2.4022953E+01	5.5519321E+01
191	0	8.9857363E+00	3.5141589E+01	283	0	2.6623025E+01	5.7012123E+01
192	0	1.1888523E+01	3.6933032E+01	284	0	2.9207814E+01	5.8567220E+01
193	0	1.4740822E+01	3.8770624E+01	285	0	3.1773039E+01	6.0182361E+01
194	0	1.7538804E+01	4.0652456E+01	286	0	3.4322798E+01	6.1860000E+01
195	0	2.0301789E+01	4.2572770E+01	287	0	3.6846315E+01	6.3605978E+01
196	0	2.3022566E+01	4.4548736E+01	288	0	3.9328544E+01	6.5429376E+01
197	0	2.5705485E+01	4.6573161E+01	289	0	4.1722626E+01	6.7458020E+01
198	0	2.8345771E+01	4.8662334E+01				
199	0	3.0944860E+01	5.0808630E+01				
200	0	3.3501733E+01	5.3023334E+01				
201	0	3.6022184E+01	5.5300137E+01				
202	0	3.8507567E+01	5.7646213E+01				
203	0	4.0952434E+01	6.0062666E+01				
204	0	4.3311712E+01	6.2567786E+01				
205	0	0.0000000E+00	3.3000000E+01				
206	0	2.9990984E+00	3.4415606E+01				
207	0	5.9836854E+00	3.5953968E+01				
208	0	8.8964730E+00	3.7589404E+01				
209	0	1.1753717E+01	3.9280851E+01				
210	0	1.4550406E+01	4.1013020E+01				
211	0	1.7319355E+01	4.2772638E+01				
212	0	2.0052728E+01	4.4585719E+01				
213	0	2.2753785E+01	4.6440417E+01				
214	0	2.5419533E+01	4.8356730E+01				
215	0	2.8048448E+01	5.0326085E+01				
216	0	3.0640137E+01	5.2361928E+01				
217	0	3.3196165E+01	5.4457383E+01				
218	0	3.5719502E+01	5.6620295E+01				
219	0	3.8213923E+01	5.8846829E+01				
220	0	4.0667834E+01	6.1155497E+01				
221	0	4.3033486E+01	6.3567571E+01				
222	0	0.0000000E+00	3.5750000E+01				
223	0	2.9915370E+00	3.7060676E+01				
224	0	5.9186413E+00	3.8520680E+01				
225	0	8.7799726E+00	4.0068967E+01				
226	0	1.1562214E+01	4.1658614E+01				
227	0	1.4326193E+01	4.3258087E+01				
228	0	1.7063956E+01	4.4911617E+01				
229	0	1.9774309E+01	4.6597984E+01				
230	0	2.2458059E+01	4.8344086E+01				
231	0	2.5108940E+01	5.0138088E+01				
232	0	2.7729122E+01	5.1996385E+01				
233	0	3.0315569E+01	5.3911483E+01				
234	0	3.2871853E+01	5.5892630E+01				
235	0	3.5400091E+01	5.7933854E+01				
236	0	3.7902109E+01	6.0043572E+01				
237	0	4.0368160E+01	6.2237992E+01				
238	0	4.2738939E+01	6.4562657E+01				
239	0	0.0000000E+00	3.8500000E+01				
240	0	2.9567373E+00	3.9732753E+01				
241	0	5.8323502E+00	4.1136027E+01				
242	0	8.5827242E+00	4.2596898E+01				
243	0	1.1327629E+01	4.4033162E+01				
244	0	1.4062651E+01	4.5529632E+01				
245	0	1.6773104E+01	4.7048807E+01				
246	0	1.9467944E+01	4.8626584E+01				
247	0	2.2132767E+01	5.0246910E+01				
248	0	2.4774686E+01	5.1928785E+01				
249	0	2.7385372E+01	5.3664476E+01				
250	0	2.9970186E+01	5.5464401E+01				
251	0	3.2527399E+01	5.7323107E+01				
252	0	3.5061334E+01	5.9246021E+01				
253	0	3.7571250E+01	6.1232767E+01				
254	0	4.0048422E+01	6.3311894E+01				
255	0	4.2426901E+01	6.5546831E+01				
256	0	0.0000000E+00	4.1250000E+01				
257	0	2.9188950E+00	4.2471125E+01				
258	0	5.6167159E+00	4.3838785E+01				
259	0	8.3229004E+00	4.5102606E+01				
260	0	1.1053039E+01	4.6444114E+01				
261	0	1.3754662E+01	4.7796451E+01				
262	0	1.6455257E+01	4.9207197E+01				
263	0	1.9126235E+01	5.0655849E+01				
264	0	2.1783140E+01	5.2162282E+01				
265	0	2.4411012E+01	5.3719635E+01				
266	0	2.7018846E+01	5.5338194E+01				
267	0	2.9600484E+01	5.7014810E+01				

ELEments

1	0	1	1	2	19	18
2	0	1	2	3	20	19
3	0	1	3	4	21	20
4	0	1	4	5	22	21
5	0	1	5	6	23	22
6	0	1	6	7	24	23
7	0	1	7	8	25	24
8	0	1	8	9	26	25
9	0	1	9	10	27	26
10	0	1	10	11	28	27
11	0	1	11	12	29	28
12	0	1	12	13	30	29
13	0	1	13	14	31	30
14	0	1	14	15	32	31
15	0	1	15	16	33	32
16	0	1	16	17	34	33
17	0	1	17	18	35	34
18	0	1	18	19	36	35
19	0	1	19	20	37	36
20	0	1	20	21	38	37
21	0	1	21	22	39	38
22	0	1	22	23	40	39
23	0	1	23	24	41	40
24	0	1	24	25	42	41
25	0	1	25	26	43	42
26	0	1	26	27	44	43
27	0	1	27	28	45	44
28	0	1	28	29	46	45
29	0	1	29	30	47	46
30	0	1	30	31	48	47
31	0	1	31	32	49	48
32	0	1	32	33	50	49
33	0	1	33	34	51	50
34	0	1	34	35	52	51
35	0	1	35	36	53	52
36	0	1	36	37	54	53
37	0	1	37	38	55	54
38	0	1	38	39	56	55
39	0	1	39	40	57	56
40	0	1	40	41	58	57
41	0	1	41	42	59	58
42	0	1	42	43	60	59
43	0	1	43	44	61	60
44	0	1	44	45	62	61
45	0	1	45	46	63	62
46	0	1	46	47	64	63
47	0	1	47	48	65	64
48	0	1	48	49	66	65
49	0	1	49	50	67	66
50	0	1	50	51	68	67
51	0	1	51	52	69	68
52	0	1	52	53	70	69
53	0	1	53	54	71	70
54	0	1	54	55	72	71
55	0	1	55	56	73	72
56	0	1	56	57	74	73
57	0	1	57	58	75	74
58	0	1	58	59	76	75
59	0	1	59	60	77	76
60	0	1	60	61	78	77
61	0	1	61	62	79	78
62	0	1	62	63	80	79
63	0	1	63	64	81	80
64	0	1	64	65	82	81
65	0	1	65	66	83	82
66	0	1	66	67	84	83
67	0	1	67	68	85	84
68	0	1	68	69	86	85
69	0	1	69	70	87	86
70	0	1	70	71	88	87
71	0	1	71	72	89	88
72	0	1	72	73	90	89

69	0	1	73	74	91	90	161	0	1	171	172	189	188
70	0	1	74	75	92	91	162	0	1	172	173	190	189
71	0	1	75	76	93	92	163	0	1	173	174	191	190
72	0	1	76	77	94	93	164	0	1	174	175	192	191
73	0	1	77	78	95	94	165	0	1	175	176	193	192
74	0	1	78	79	96	95	166	0	1	176	177	194	193
75	0	1	79	80	97	96	167	0	1	177	178	195	194
76	0	1	80	81	98	97	168	0	1	178	179	196	195
77	0	1	81	82	99	98	169	0	1	179	180	197	196
78	0	1	82	83	100	99	170	0	1	180	181	198	197
79	0	1	83	84	101	100	171	0	1	181	182	199	198
80	0	1	84	85	102	101	172	0	1	182	183	200	199
81	0	1	86	87	104	103	173	0	1	183	184	201	200
82	0	1	87	88	105	104	174	0	1	184	185	202	201
83	0	1	88	89	106	105	175	0	1	185	186	203	202
84	0	1	89	90	107	106	176	0	1	186	187	204	203
85	0	1	90	91	108	107	177	0	1	188	189	206	205
86	0	1	91	92	109	108	178	0	1	189	190	207	206
87	0	1	92	93	110	109	179	0	1	190	191	208	207
88	0	1	93	94	111	110	180	0	1	191	192	209	208
89	0	1	94	95	112	111	181	0	1	192	193	210	209
90	0	1	95	96	113	112	182	0	1	193	194	211	210
91	0	1	96	97	114	113	183	0	1	194	195	212	211
92	0	1	97	98	115	114	184	0	1	195	196	213	212
93	0	1	98	99	116	115	185	0	1	196	197	214	213
94	0	1	99	100	117	116	186	0	1	197	198	215	214
95	0	1	100	101	118	117	187	0	1	198	199	216	215
96	0	1	101	102	119	118	188	0	1	199	200	217	216
97	0	1	103	104	121	120	189	0	1	200	201	218	217
98	0	1	104	105	122	121	190	0	1	201	202	219	218
99	0	1	105	106	123	122	191	0	1	202	203	220	219
100	0	1	106	107	124	123	192	0	1	203	204	221	220
101	0	1	107	108	125	124	193	0	1	205	206	223	222
102	0	1	108	109	126	125	194	0	1	206	207	224	223
103	0	1	109	110	127	126	195	0	1	207	208	225	224
104	0	1	110	111	128	127	196	0	1	208	209	226	225
105	0	1	111	112	129	128	197	0	1	209	210	227	226
106	0	1	112	113	130	129	198	0	1	210	211	228	227
107	0	1	113	114	131	130	199	0	1	211	212	229	228
108	0	1	114	115	132	131	200	0	1	212	213	230	229
109	0	1	115	116	133	132	201	0	1	213	214	231	230
110	0	1	116	117	134	133	202	0	1	214	215	232	231
111	0	1	117	118	135	134	203	0	1	215	216	233	232
112	0	1	118	119	136	135	204	0	1	216	217	234	233
113	0	1	120	121	138	137	205	0	1	217	218	235	234
114	0	1	121	122	139	138	206	0	1	218	219	236	235
115	0	1	122	123	140	139	207	0	1	219	220	237	236
116	0	1	123	124	141	140	208	0	1	220	221	238	237
117	0	1	124	125	142	141	209	0	1	222	223	240	239
118	0	1	125	126	143	142	210	0	1	223	224	241	240
119	0	1	126	127	144	143	211	0	1	224	225	242	241
120	0	1	127	128	145	144	212	0	1	225	226	243	242
121	0	1	128	129	146	145	213	0	1	226	227	244	243
122	0	1	129	130	147	146	214	0	1	227	228	245	244
123	0	1	130	131	148	147	215	0	1	228	229	246	245
124	0	1	131	132	149	148	216	0	1	229	230	247	246
125	0	1	132	133	150	149	217	0	1	230	231	248	247
126	0	1	133	134	151	150	218	0	1	231	232	249	248
127	0	1	134	135	152	151	219	0	1	232	233	250	249
128	0	1	135	136	153	152	220	0	1	233	234	251	250
129	0	1	137	138	155	154	221	0	1	234	235	252	251
130	0	1	138	139	156	155	222	0	1	235	236	253	252
131	0	1	139	140	157	156	223	0	1	236	237	254	253
132	0	1	140	141	158	157	224	0	1	237	238	255	254
133	0	1	141	142	159	158	225	0	1	239	240	257	256
134	0	1	142	143	160	159	226	0	1	240	241	258	257
135	0	1	143	144	161	160	227	0	1	241	242	259	258
136	0	1	144	145	162	161	228	0	1	242	243	260	259
137	0	1	145	146	163	162	229	0	1	243	244	261	260
138	0	1	146	147	164	163	230	0	1	244	245	262	261
139	0	1	147	148	165	164	231	0	1	245	246	263	262
140	0	1	148	149	166	165	232	0	1	246	247	264	263
141	0	1	149	150	167	166	233	0	1	247	248	265	264
142	0	1	150	151	168	167	234	0	1	248	249	266	265
143	0	1	151	152	169	168	235	0	1	249	250	267	266
144	0	1	152	153	170	169	236	0	1	250	251	268	267
145	0	1	154	155	172	171	237	0	1	251	252	269	268
146	0	1	155	156	173	172	238	0	1	252	253	270	269
147	0	1	156	157	174	173	239	0	1	253	254	271	270
148	0	1	157	158	175	174	240	0	1	254	255	272	271
149	0	1	158	159	176	175	241	0	1	256	257	274	273
150	0	1	159	160	177	176	242	0	1	257	258	275	274
151	0	1	160	161	178	177	243	0	1	258	259	276	275
152	0	1	161	162	179	178	244	0	1	259	260	277	276
153	0	1	162	163	180	179	245	0	1	260	261	278	277
154	0	1	163	164	181	180	246	0	1	261	262	279	278
155	0	1	164	165	182	181	247	0	1	262	263	280	279
156	0	1	165	166	183	182	248	0	1	263	264	281	280
157	0	1	166	167	184	183	249	0	1	264	265	282	281
158	0	1	167	168	185	184	250	0	1	265	266	283	282
159	0	1	168	169	186	185	251	0	1	266	267	284	283
160	0	1	169	170	187	186	252	0	1	267	268	285	284

```

253 0 1 268 269 286 285
254 0 1 269 270 287 286
255 0 1 270 271 288 287
256 0 1 271 272 289 288

BOUNDary conditions
  1 0 1 1
 18 0 1 1
 35 0 1 1
 52 0 1 1
 69 0 1 1
 86 0 1 1
103 0 1 1
120 0 1 1
137 0 1 1
154 0 1 1
171 0 1 1
188 0 1 1
205 0 1 1
222 0 1 1
239 0 1 1
256 0 1 1
273 0 1 1

FORCe conditions
 17 0 0.000000E+00 3.125000E+00
 34 0 0.000000E+00 6.250000E+00
 51 0 0.000000E+00 6.250000E+00
 68 0 0.000000E+00 6.250000E+00
 85 0 0.000000E+00 6.250000E+00
102 0 0.000000E+00 6.250000E+00
119 0 0.000000E+00 6.250000E+00
136 0 0.000000E+00 6.250000E+00
153 0 0.000000E+00 6.250000E+00
170 0 0.000000E+00 6.250000E+00
187 0 0.000000E+00 6.250000E+00
204 0 0.000000E+00 6.250000E+00
221 0 0.000000E+00 6.250000E+00
238 0 0.000000E+00 6.250000E+00
255 0 0.000000E+00 6.250000E+00
272 0 0.000000E+00 6.250000E+00
289 0 0.000000E+00 3.125000E+00

para
k=1.e8
u=80.0

mate,1
user,16
neoh material k u
pressure option 2
mixed threefield
temp current 270.0
temp reference 300.0
thermal isotropic 1.d-6

end

batch
dt,,1
prop
loop,,10
time
loop,,15
utan,,1
next
next
end

inte

stop

bloc
cart 3 8
1 2.25 0
2 3 0
3 3 1
4 2.25 1

bloc
cart 12 4
1 0 1
2 3 1
3 3 1.5
4 0 1.5

eboun
2,0,0,1

csurf
linear
1 2.25 1 -100
2 2.25 0 -100
linear
1 0 1 -100
2 2.25 1 -100

! k = bulk modulus
! u = shear modulus

para
k=1.e4
u=1.e2

mate
user,16
neoh constitution k u
pressure option 2
mixed threefield
axis symmetric

end

tie

batch
nopr
plot,wipe
plot,mesh
plot,defo,,1
dt,,.01
prop
end
0

batch
loop,,2
time
loop,,10
utan,,1
next
plot,mesh
next
end

inte

stop

```

C Input file for Example 6.3

B Input file for Example 6.2

```

feap * Inflation of a bi-material band
0,0,0,2,2,4

feap * Axis-symmetric Cap
0,0,1,2,2,4

bloc
cart 4 16 0 0 1
1 3 0
2 3.5 0

```

```

3 3.5 2
4 3 2
6 3.8 1
8 3.3 1

bloc
cart 4 4 0 0 2
1 3.5 0
2 4 0
3 4 0.5
4 3.725 0.5
8 3.6312 0.25

bloc
cart 4 4 0 0 2
1 3.725 1.5
2 4 1.5
3 4 2
4 3.5 2
8 3.6312 1.75

eboun
2 0 0 1

csur
quadratic
1 3 2 -25
2 3 0 -25
3 3.3 1 -25

orthotropic element angles !over-rides default on material card
elem 65 0.0
elem 66 0.0
elem 67 0.0
elem 68 0.0
elem 69 0.0
elem 70 0.0
elem 71 0.0
elem 72 0.0
elem 73 0.0
elem 74 0.0
elem 75 0.0
elem 76 0.0
elem 77 0.0
elem 78 0.0
elem 79 0.0
elem 80 0.0
elem 81 1.5
elem 82 1.5
elem 83 1.5
elem 84 1.5
elem 85 1.5
elem 86 1.5
elem 87 1.5
elem 88 1.5
elem 89 1.5
elem 90 1.5
elem 91 1.5
elem 92 1.5
elem 93 1.5
elem 94 1.5
elem 95 1.5
elem 96 1.5

para
k=1.e4
u=80.0

mate 1
user,16
neoh constitution k u
pressure option 2.d0
mixed threefield
temperature current 270.0
temperature reference 350.0
thermal isotropic 2.d-6
axis symmetric

mate 2
user,16
transverse isotropic 12100 10200 10100 10000 500 0.0
temperature current 270.0
temperature reference 350.0
thermal transverse 1.d-6 1.5d-6
axis symmetric

end

tie

batch
loop,,10
utan,,1
next
end

inte

stop

!eap * Inflation of a bi-material band orthotropic
0,0,0,2,2,4

bloc
cart 4 16 0 0 1
1 3 0
2 3.5 0
3 3.5 2
4 3 2
6 3.8 1
8 3.3 1

bloc
cart 4 4 0 0 2
1 3.5 0
2 4 0
3 4 0.5
4 3.725 0.5
8 3.6312 0.25

bloc
cart 4 4 0 0 2
1 3.725 1.5
2 4 1.5
3 4 2
4 3.5 2
8 3.6312 1.75

eboun
2 0 0 1

csur
quadratic
1 3 2 -25
2 3 0 -25
3 3.3 1 -25

orthotropic element angles !over-rides default on material card
elem 65 0.0
elem 66 0.0
elem 67 0.0
elem 68 0.0
elem 69 0.0
elem 70 0.0
elem 71 0.0
elem 72 0.0
elem 73 0.0
elem 74 0.0
elem 75 0.0
elem 76 0.0
elem 77 0.0
elem 78 0.0
elem 79 0.0
elem 80 0.0
elem 81 1.5
elem 82 1.5
elem 83 1.5
elem 84 1.5
elem 85 1.5
elem 86 1.5
elem 87 1.5
elem 88 1.5
elem 89 1.5
elem 90 1.5
elem 91 1.5
elem 92 1.5
elem 93 1.5
elem 94 1.5

```

D Input file for Example 6.4

```
elem 95 1.5  
elem 96 1.5
```

```
para  
k=1.e4  
u=80.0
```

```
mate 1  
user,16  
nech constitution k u  
pressure option 2.d0  
mixed threefield  
temperature current 270.0  
temperature reference 350.0  
thermal isotropic 2.d-6  
axis symmetric
```

```
mate 2  
user,16  
orthotropic stvk 12100 10200 10300 10100 10000 10500 500 300 400 0.0  
temperature current 270.0  
temperature reference 350.0  
thermal orthotropic 1.d-6 1.5d-6 2.d-6  
axis symmetric
```

```
end
```

```
tie
```

```
inte  
stop
```

E Element 16 Input Options

E.1 Material Selection

Neo-Hookean

To use a neo-hookean solid one enters the following card

```
neohookean isotropic kappa mu
```

where `kappa` and `mu` are the numerical values of the bulk modulus κ and the shear modulus μ .

Transverse Isotropy

To use a transverse isotropic Saint-Venant Kirchhoff solid one enters the following card

```
transverse isotropy C11 C22 C12 C23 C44 theta
```

where `C11`, `C22`, `C12`, `C23`, and `C44` are the corresponding stiffness entries in the `C` stiffness matrix. The remaining entries are automatically computed. The 1-direction corresponds to the normal to the plane of transverse isotropy in the reference configuration \mathbf{P} . The angle that the mapped vector \mathbf{p} make with the horizontal is taken as `theta`. If the `orthotropic angles` card in the `MESH` has been set then `theta` is ignored and the values from the `orthotropic angles MESH` card are used.

Orthotropy

To use an orthotropic Saint-Venant Kirchhoff solid one enters the following card

```
orthotropic stvk C11 C22 C33 C12 C23 C13 C44 C55 C66 theta
```

where `C11`, `C22`, `C33`, `C12`, `C23`, `C13`, `C44`, `C55`, and `C66` are the corresponding stiffness entries in the `C` stiffness matrix. The 1-direction corresponds to the orthotropic axis defined by the reference configuration vector \mathbf{P} . The angle that the mapped vector \mathbf{p} make with the horizontal is taken as `theta`. If the `orthotropic angles` card in the `MESH` has been set then `theta` is ignored and the values from the `orthotropic angles MESH` card are used.

E.2 Mixed Options

For the neo-hookean material one has the option of choosing a two-field or three-field formulation. Note that the two-field formulation is only available with a quadratic pressure term and does not include thermal effects. The choice is made by including the card:

```
mixed twofield
```

or

```
mixed threefield
```

E.3 Pressure Function

The pressure function for the neo-hookean model can be the simple quadratic model or the one described in this report. Note that the pressure model in this report does not function with the two field formulation. Also note that the quadratic model does not function with temperature changes. The models are selected by using the following cards:

```
pressure option 1
```

and

```
pressure option 2
```

Pressure option 1 corresponds to the quadratic model and pressure option 2 corresponds to the quadratic-log model described in this report.

For greatest flexibility the neo-hookean model should be used with the three field formulation and pressure option 2. The other options are mainly included for historical purposes.

E.4 Thermal Options

The thermal options are available for the anisotropic models and isotropic model when using a three field formulation with pressure option 2. The thermal expansion coefficients are set using the following cards depending upon the material model:

```
thermal isotropic alpha
```

or

thermal transverse alpha-p alpha-plane

or

thermal orthotropic alpha-p alpha-q alpha-*

alpha is the numerical value of the isotropic coefficient of thermal expansion. For transversely isotropic materials alpha-p is the thermal expansion coefficient in the material direction P and alpha-plane is the thermal expansion coefficient in the "isotropic" plane. For orthotropic materials alpha-p is the thermal expansion coefficient in the material direction P , alpha-q is the thermal expansion coefficient in the material direction Q , and alpha-* is the thermal expansion coefficient in the third orthotropic direction.

The reference temperature is specified using the following card:

temperature reference T_0

where T_0 is the numerical value of the reference temperature T_0 . The current temperature is specified using the following card:

temperature current T

where T is the numerical value of the current temperature T .

E.5 Mass properties

The dynamical options are not available with this element. However the mass matrix is available for generalized eigenvalue analysis. Options are specified on the following cards:

density material rho

where rho is the mass density of the material ρ . The mass may be lumped or chosen to be consistent by specifying one of the following two cards:

mass lumped

or

mass consistent

E.6 Anisotropic Angles

The inclination of the vector \mathbf{p} in the transverse isotropy and orthotropy models can be specified as a single value for all elements of a particular material set or can be over-ridden using the following card in the MESH input.

```
orthotropic angles  
elem elem-# angle  
elem elem-# angle  
elem elem-# angle  
<blank line to terminate input>
```

`elem-#` is the numerical number of the element for which the angle is to be specified. `angle` is the angle to be assigned to the given element number. Every element for which an angle is to be specified must be included. A blank line terminates the entries.